Obrabotka metallov (tekhnologiya, oborudovanie, instrumenty) = Metal Working and Material Science. 2024 vol. 26 no. 4 pp. 75–91
ISSN: 1994-6309 (print) / 2541-819X (online)
DOI: 10.17212/1994-6309-2024-26.4-75-91

NSTU NETI

Obrabotka metallov -
Metal Working and Material Science

Journal homepage: http://journals.nstu.ru/obrabotka_metallov

Assessment of the quality and mechanical properties of metal layers from low-carbon steel obtained by the WAAM method with the use of additional using additional mechanical and ultrasonic processing

Yulia Karlina [1, a, *], *Vladimir Konyukhov* [2, b], *Tatiana Oparina* [2, c]

[1] National Research Moscow State University of Civil Engineering, 26 Yaroslavskoe Shosse, Moscow, 129337, Russian Federation
[2] Irkutsk National Research Technical University, 83 Lermontova str., Irkutsk, 664074, Russian Federation

[a] https://orcid.org/0000-0001-6519-561X, jul.karlina@gmail.com; [b] https://orcid.org/0000-0001-9137-9404, konyukhov_vyu@mail.ru;
[c] https://orcid.org/0000-0002-9062-6554, martusina2@yandex.ru

ARTICLE INFO

Article history:
Received: 14 September 2024
Revised: 08 October 2024
Accepted: 17 October 2024
Available online: 15 December 2024

Keywords:
Additive Manufacturing
Wire and arc additive manufacturing
WAAM
Wire
Structure
Ultrasonic hardening
Hardness
Yield strength
Pores
Gas

ABSTRACT

Introduction. Additive manufacturing is a technology that enables three-dimensional (3D) components to be printed layer by layer according to digital models. Completely different from traditional manufacturing methods such as casting, forging, and machining, additive manufacturing is a near net shape manufacturing process that can greatly enhance design freedom and reduce manufacturing runtime. The material processing challenges in Wire and Arc Additive Manufacturing (*WAAM*) are related to achieving performance metrics related to geometric, physical, and material properties. Tight tolerances and stringent surface integrity requirements cannot be achieved by utilizing stand-alone *AM* technologies. Therefore, *WAAM* parts typically require some post-processing to meet requirements related to surface finish, dimensional tolerances and mechanical properties. It is therefore not surprising that the integration of *AM* with post-processing technologies into single and multi-setup machining solutions, commonly referred to as hybrid *AM*, has become a very attractive proposition for industry. **The purpose of the work** is to evaluate the quality and mechanical properties of the resulting metal layers of mild steel by *WAAM* method using additional mechanical and ultrasonic processing. **Research Methods.** To conduct the experiments, a set of welding equipment was used — a single-phase inverter device *KEMPPI Kempomat 1701*, designed for welding with wire in shielding gases. A mixture of argon and carbon dioxide (80 % argon and 20 % CO_2) was used as a shielding gas. *SV-08G2S* (0.8 C-2 Mg-Si) wire was used as the surfacing material. A plate made of steel *St3* with overall dimensions 150×100×5 mm was used as a base for surfacing. The surface of the plate before surfacing was thoroughly cleaned from the layer of oxides, oil, rust and other contaminants. For this purpose mechanical cleaning of the surface was used with *BOSCH* abrasive wheel with a diameter of 125 mm diameter and a grit size of 120. Before surfacing the surface of the product was degreased with white spirit. The gas flow rate was set at 8 dm^3/min. To select the optimal wire feed rate and volt-ampere characteristic, surfacing was performed at each adjustment step of wire feed rate, and voltage. Mechanical statistical tensile tests, chemical composition analysis and metallographic studies were also performed. **Results and Discussion.** Gas porosity is a typical defect that occurs during the *WAAM* process and should be eliminated because it adversely affects the mechanical properties. Initially, gas porosity leads to a reduction in the mechanical strength of the part due to damage from microcrack formation. In addition, it often causes the surfaced layer to have worse fatigue properties due to the spatial distribution of different shape and size structures. In our experiments we found that a wire feed speed range of 5–6 m/min is optimal. Increasing the flow rate of shielding gas in the range of 8–14 l/min allows reducing porosity in the surfaced metal to almost zero. The mechanical properties of the surfaced beads show that the average value of yield strength after machining is higher than that of unprocessed specimens. The data obtained from these experiments are in good agreement with those reported in the literature. The presented results can be used in real *WAAM* technological processes.

For citation: Karlina Yu.I., Konyukhov V.Yu., Oparina T.A. Assessment of the quality and mechanical properties of metal layers from low-carbon steel obtained by the WAAM method with the use of additional using additional mechanical and ultrasonic processing. *Obrabotka metallov (tekhnologiya, oborudovanie, instrumenty) = Metal Working and Material Science*, 2024, vol. 26, no. 4, pp. 75–91. DOI: 10.17212/1994-6309-2024-26.4-75-91. (In Russian).

*** Corresponding author**
Karlina Yulia I., Ph.D. (Engineering), Research Associate
National Research Moscow State Construction University,
Yaroslavskoe shosse, 26,
129337, Moscow, Russian Federation
Tel.: +7 914 879-85-05, **e-mail:** jul.karlina@gmail.com

Introduction

Advances in additive manufacturing (*AM*) technology have expanded its application areas, and *AM* is becoming a viable option for producing fully functional metal parts [1–3]. In fact, metal *AM* is currently being applied in various industries [3–5]. One of the *AM* methods is Wire and Arc Additive Manufacturing (*WAAM*). Among all the existing *AM* methods, *WAAM* is known to be a relatively low-cost method that provides the highest surfacing rates [1–5]. Using this technology, the surfacing process is carried out in the open air using a robotic arm with a fixed welding torch, with a localized shielded area [5–15].

An important challenge in ensuring the structural integrity of *WAAM* components is to evaluate the impact of the welding processes integrated into the *WAAM* technology on the mechanical and fracture properties compared to those obtained from the as-deformed material. *WAAM* technology enables the creation of parts with complex topologically optimized geometries with internal cavities that are impossible to form using traditional manufacturing processes. However, in most cases, the tight tolerances and strict surface integrity requirements cannot be achieved using stand-alone *AM* technologies. Therefore, *WAAM* parts usually require some post-processing to meet the requirements related to surface finish, dimensional tolerances and mechanical properties.

Most of the literature on additive manufacturing describes the integration of AM with post-processing technologies into single- or multi-tool processing solutions, commonly referred to as hybrid AM.

Most of the work devoted to additive manufacturing integrates *AM* with post-processing technologies into single- or multi-setup processing solutions, commonly referred to as hybrid *AM*. Hybrid *AM* has become a very attractive proposition for the industry, which has increased the amount of *R&D* work [5–15] aimed at developing this direction. The combination of additive and subtractive methods offers a possible method to overcome this inherent problem of the process. It is also important to understand, and has been shown in numerous studies [10–18], that *AM* parts may contain voids or pores due to trapped gas or incomplete fusion during the printing process, which can weaken the structural integrity of the component.

The works [4–9] point to an example that has been implemented in the Shape Deposition Manufacturing (*SDM*) process at Stanford University and the Controlled Material Buildup (*CMB*) process developed at IPT Aachen. In these processes, each layer is applied as a near-net shape using a thermal spray process, essentially laser cladding. The layer is then further shaped by *CNC* milling to the net shape before the next layer is added. In *SDM* processes, the top and side surfaces of each layer are machined and then protected by adding a copper support structure. This support structure is then removed using an etching process when the part is complete.

In the work [4], the authors developed a similar approach, 3D welding and milling, using *WAAM* instead of laser cladding for faster and more cost-effective surfacing of individual beads. In the 3D welding and milling process, conventional gas metal arc welding is used to surface individual beads next to each other. Depending on the welding parameters such as speed and power, the bead thickness varies from 0.5 to 1.5 mm. When applying a layer, its upper surface is machined to obtain a smooth surface of a certain thickness for further application. Combining this process with face milling gives a clear advantage in setting the layer thickness from 0.1 to 1.0 mm. Once the deposition and face milling sequence is completed, a surface finishing treatment is applied in the same setup to remove the remaining steps on the surface and improve the near-net shape accuracy of the metal part. Until now, the mechanical properties and microstructure of *WAAM* carbon steels have not been comprehensively characterized.

To fill this gap in knowledge, the authors of [19–22] conducted a comprehensive series of tensile tests on plates made of normal and high-strength *WAAM* steel; the microstructure of both steel grades was also investigated. In the works [23, 24], the fracture toughness of deposited walls made of low-carbon steel was investigated, and the advantage of the *WAAM* method was demonstrated.

Some applications of the *WAAM* process are summarized in [22, 23] regarding the welding heat source used by the researchers.

Some researchers have tried to use the gas metal arc welding (*GMAW*) process [23, 24] for *WAAM* as the main deposition tool due to its advantages such as relatively low metal spatter, independent control of the heat source and wire feed system combined with additional machining [25]. Other related processes in which a plasma torch is used instead of *GTAW* are Hybrid Plasma Deposition and Milling (*HPDM*) and Micro Plasma Arc Welding rapid prototyping (*MPAW*) [26, 27]. In all the metal deposition processes discussed above, precise layer height control remains a challenge due to the wavy nature of multi-pass deposition. To obtain components with precise layer thickness, some researchers have combined milling and deposition [4–6, 25]. These hybrid processes perform a surface milling operation after each layer to ensure *z*-accuracy. 3D welding and milling developed by [4, 5] combine *GMAW* deposition with a conventional milling process to produce injection molding inserts [7–12].

In the works [28–30] it is proposed to additionally use ultrasonic processing of products obtained by *WAAM* technology. According to the authors, this will improve the mechanical properties of the grown products. Many parameters of ultrasonic additional processing in the *WAAM* process have not yet been optimized and depend on the type of equipment, frequency, amplitude, etc.

At the same time, the integration of traditional subtractive technologies with *WAAM* can provide improved material and energy savings compared to pure subtractive approaches. In fact, *WAAM* components typically exhibit high structural integrity when the process parameters are optimized, so only machining operations need to be performed. In addition, very little surface deformation depth is expected with the hybrid technology. The synergistic integration of the surfacing unit with the *CNC* machine, regardless of its brand and age, is a key aspect in the hybrid technology. The integration should be done in a way that surfacing can act as an additional function without disturbing other capabilities of the *CNC* machine. During the integration, changes to the mechanical and electrical systems are made without the need for any proprietary information from the machine manufacturer or the control system designer. There are mechanical challenges: the first is to mount the welding torch on the side of the spindle so that surfacing is controlled through the same *CNC* controller; the second is to select a suitable mechanism to remove the excess heat generated during welding; the third is to take appropriate precautions to protect the machine components from accidental splashes. Electrical and control problems arise separately:

1) switching on/off the welding and surfacing unit via the *CNC* program;
2) simple and fast switching between surfacing mode and normal *CNC* mode;
3) elimination of any direct electrical contact between the *CNC* controller and the welding unit.

It is important to understand that serial equipment for the implementation of complex (hybrid additive technology) is not yet manufactured, and all work performed in this area is associated with the modernization of *CNC* machines, which is not always justified from an economic point of view. A relatively simple methodological point of view and minimal financial costs for equipment is an approach based on the separate use of *WAAM* technology with other processing methods that are available for a wider range of studies, in order to study the properties of the obtained materials. This paper presents a study of the characteristics of metal processing applied by the *WAAM* method with additional mechanical and ultrasonic processing.

The ***aim of the work*** is to evaluate the quality and mechanical properties of the obtained metal layers from low-carbon steel using the *WAAM* method with the use of additional mechanical and ultrasonic processing.

Materials and research methods

A single-phase inverter device *KEMPPI Kempomat* 1701 was used as a power source for mechanized surfacing in a protective gas environment. A mixture of argon (80 %) and CO_2 (20 %) was used as a shielding gas. Welding wire *Sv-08G2S* (*0.08 C-2 Mn-Si*) with a copper coating of 1.0 mm in diameter was used. The parameters of the layer growth process (Fig. 1, *a*) were determined to ensure optimal productivity and cooling time between successive layer depositions. The number of passes was determined to be 5. After each pass, mechanical processing of the surface of the surfaced bead was carried out. Then, visual inspection was carried out and a magnifying glass (ten-power magnification) was used to assess the surface quality. After the inspection, a new layer was surfaced (Fig. 1, *b*).

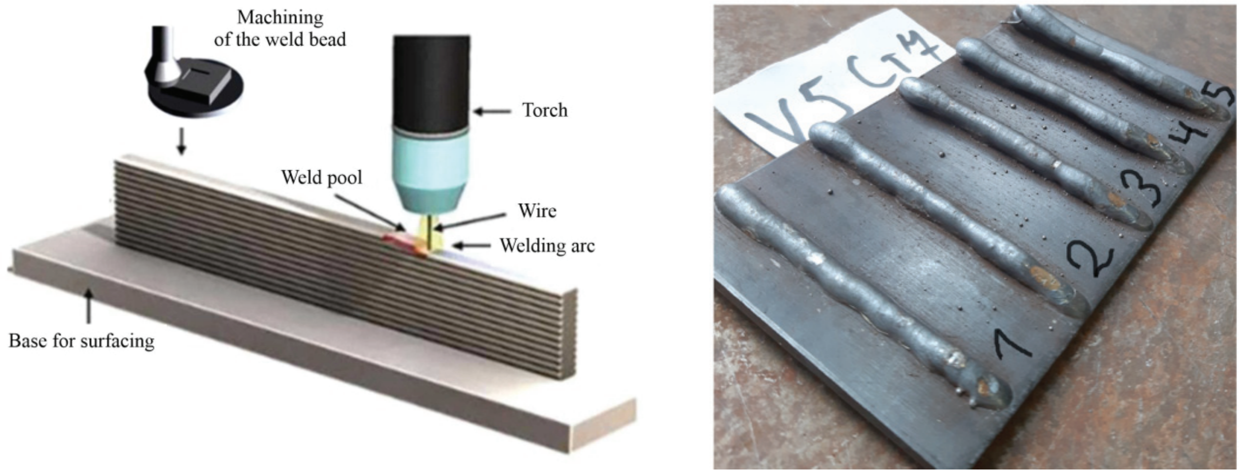

a *b*

Fig. 1. Schematic diagram of the bead surfacing process (*a*) and a plate with surfaced beads (*b*)

The variable parameters were the wire feed and the shielding gas consumption. The gas consumption during the experiments was selected in the range of 8–12 l/min. This had to be done in order to evaluate this parameter for porosity. At the same time, other parameters, current, wire feed, surfacing speed were constant. Ultrasonic processing was carried out on the last surfacing layer for 1, 5, 10, 15 minutes using the *Shmel Mg* unit.

Tensile tests were carried out in accordance with *GOST 1497-84*. A total of 3 test pieces were cut from a steel wall manufactured using standard *WAAM* and hybrid *WAAM*. Impact toughness (KCU) was carried out in accordance with *GOST 9454-78* and *GOST 6996*. For this purpose, 3 test pieces were cut from a steel wall manufactured using standard *WAAM* and hybrid *WAAM* and prepared. After completion of the impact bending tests, the fracture surfaces of the test pieces were examined using a *JEOL JIB-Z4500-SEM* scanning electron microscope (*SEM*) to compare the main types of failure associated with different forming technologies.

For microstructural analysis, metallographic specimens were extracted from the wall along the growth directions, polished according to standard procedures to a surface finish of 1 μm, etched with 4 % aqueous nitric acid solution and examined using an optical microscope (*MicroMed 2*). Hardness measurements were carried out at different locations and orientations of the wall, including the lower, middle and upper zones, using a *Shimadzu HBR-VU-187* microhardness tester with a load of 200 g and a dwell time of 15 s.

Research results

Fig. 2, 3 show the results of the influence of the wire feed and the shielding gas consumption on the metal porosity. The numbers **1**, **2**, **3**, **4**, **5** in Fig. 2 show the number of weld beads. Fig. 3 shows the influence of the shielding gas consumption on the porosity. It is evident that with an increase in consumption, the porosity in the weld metal decreases to zero.

Fig. 4 shows the results of the influence of mechanical cleaning after each layer of surfacing on the surface quality and the geometric dimensions of the surfaced bead. It is evident that the use of machining affects the height of the surfaced bead and the quality of the weld (Fig. 5).

The microstructure of the surfaced beads material, shown in Fig. 6, consists of polygonal ferrite (*PF*) and intergranular lamellar pearlite (*P*).

Tables 1 and 2 present the results of static tensile tests and impact bending tests. It is evident that machining increases the yield strength and endurance of the surfaced metal compared to the results without machining. The impact toughness values also differ when additional machining is used. The fractography images in Fig. 7, *b* show that the specimens without machining contain pores, which reduces the impact toughness values.

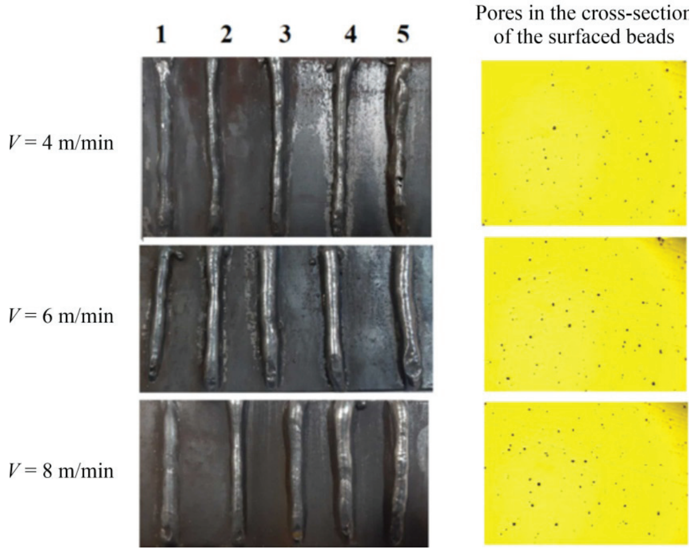

Fig. 2. Effect of wire feed on porosity across the surfaced bead cross section

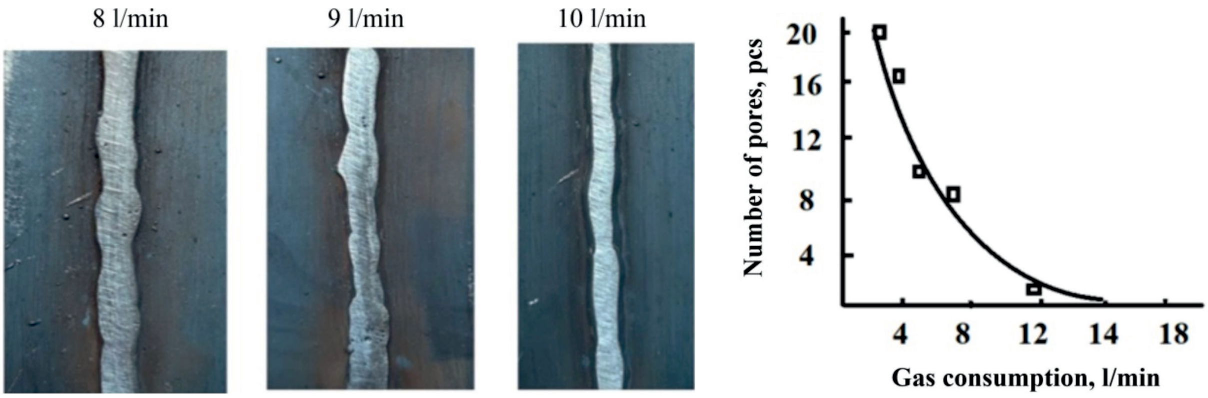

a *b*

Fig. 3. Effect of shielding gas flow rate on porosity in surfaced beads (*a*) and a graph of the dependence of the number of pores on the gas flow rate (*b*)

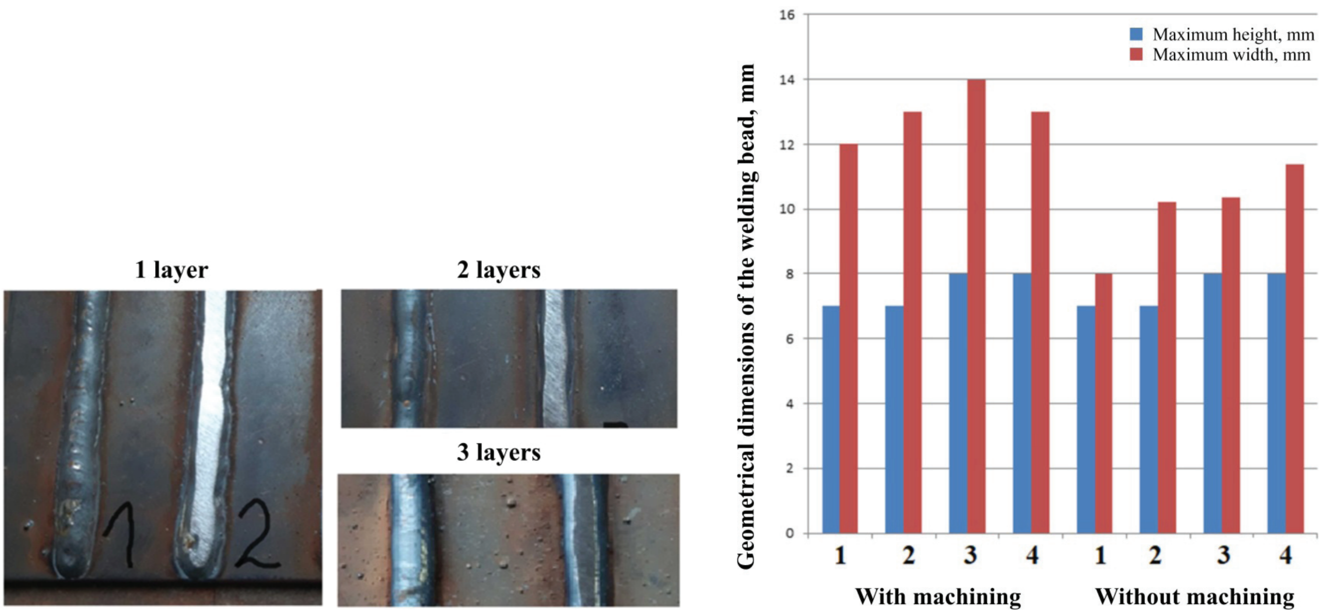

a *b*

Fig. 4. Effect of machining on the geometrical parameters of the surfaced bead depending on the number of passes (1, 2, 3, 4, 5) (*a*) and graphical representation of the dependence (*b*)

Fig. 5. Assessment of weld quality after machining after each pass

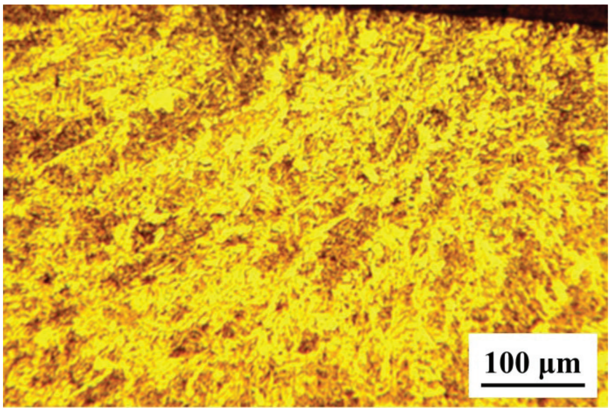

a

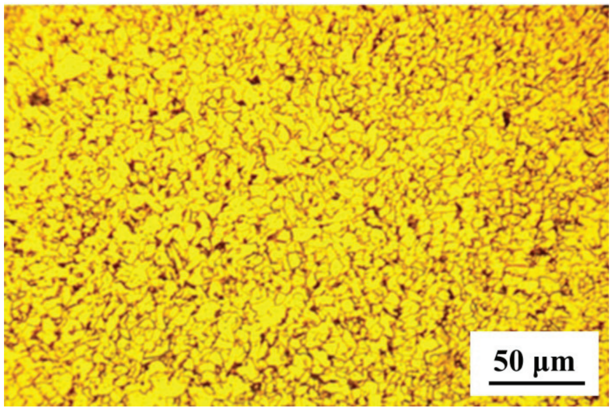

b

Fig. 6. Microstructure of metal in the joint area after tempering

Table 1

Results of static tensile tests

Specimen identification mark	Test temperature, °C	Yield strength, σ_y ($\sigma_{0,2}$) MPa	Ultimate strength, σ_u, MPa	Relative elongation, δ_5 (δ_{10}), %
1	20	364; 356; 361	474; 479; 481	16.75; 17.01; 16.82
2 with machining	20	404; 410; 412	518; 522; 527	33.25; 33.01; 32.48
Steel *0.09 C-2 Mn-Si* (*GOST*)		265	430	21
Steel *0.09 C-2 Mn-Si* (Fact)	20	275; 270; 278	435; 431; 440	22.01; 22.12; 22.34

Table 2

Results of impact bending tests

Specimen identification mark	Test temperature, °C	Geometric dimensions of the specimen			Work of fracture (KU), kg/cm	Impact strength, (KCU), J/cm^2	Note
		Width, mm	Height, mm (at the point of incision)	Cross-sectional area, cm^2			
4	20	9.95	7.94	0.790	15.6	183.5	Surfacing
5	20	9.94	7.9	0.785	14.8	194.7	
6	20	10.01	7.92	0.792	21.5	255.7	Surfacing with machining
7	20	9.96	7.95	0.791	21.2	268.3	
Steel *0.09 C-2 Mn-Si* (*GOST*)	20					Not less than 59	
Steel *0.09 C-2 Mn-Si* (Fact)	20					115	

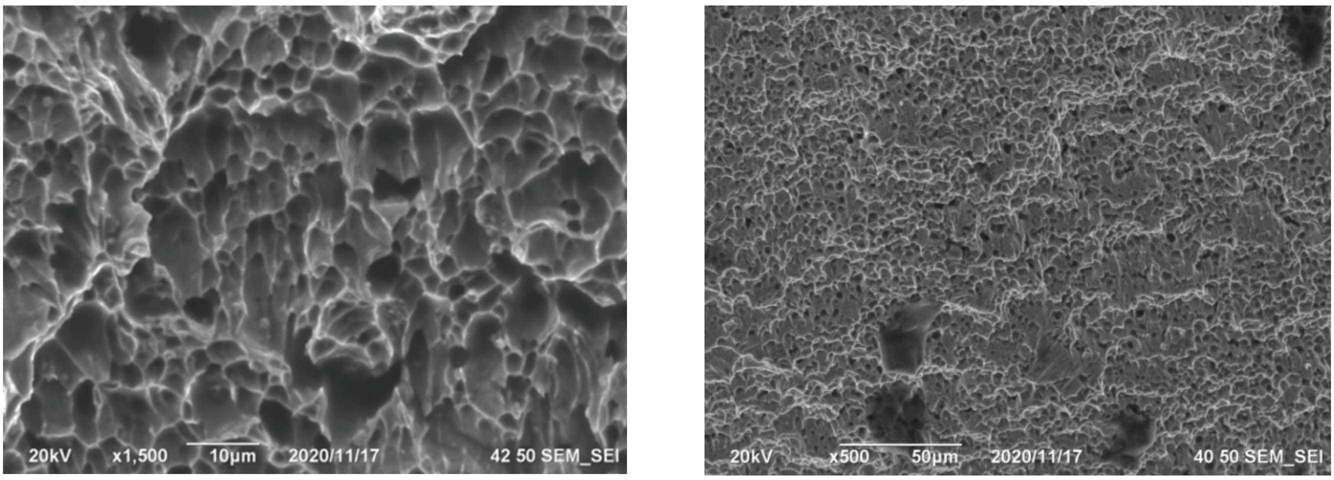

a *b*

Fig. 7. Fracture analysis of specimens with machining (*a*) and without (*b*)

The results of ultrasonic processing tests of the upper bead are shown in Fig. 8. Traces of plastic deformation are visible in the microstructure image (Fig. 8, *a*). Processing time affects the microhardness values (Fig. 8, *b*).

Research and discussion

According to numerous studies on welded arc additive manufacturing (*WAAM*) [2–10,18–28], in order to obtain excellent quality of surfaced metal without any defects, it is necessary to carefully select and implement a combination of process parameters, such as wire diameter, wire feed, travel speed, welding

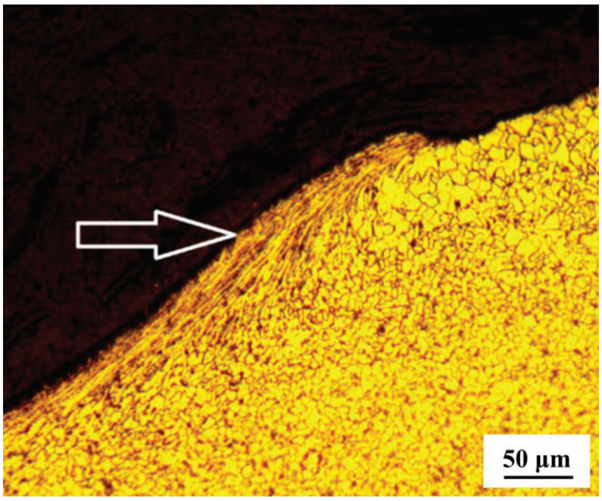

a

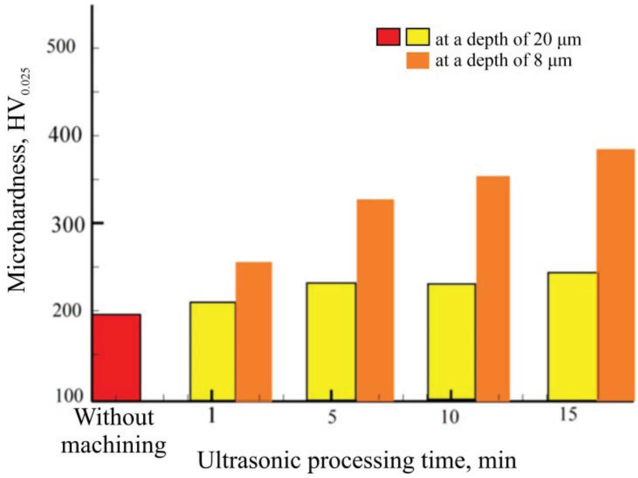

b

Fig. 8. Results of ultrasonic hardening of the top bead (*a*) and hardness distribution in the surface layer (*b*)

voltage, welding current, nozzle-to-workpiece distance, shielding gas torch angle and step distance. The main problem faced by *WAAM* is to decide whether to increase the deposition rate of the metal being deposited or to reduce the heat input distribution. This is due to the fact that the wire feed is closely related to the required heat input [15–20] for its melting. In our experiments, we found that the optimal indicator is the range of wire feed of 5–6 m/min. At the same time, we saw that with such parameters there is another factor that should be taken into account; this factor is the porosity of the weld bead (Fig. 2).

It is known that gas porosity is a typical defect that occurs in the *WAAM* process and should be eliminated because it negatively affects the mechanical properties [23, 24]. Initially, gas porosity leads to a decrease in the mechanical strength of the component due to damage from the formation of microcracks. In addition, it often leads to the fact that the deposited layer has worse fatigue properties due to the spatial distribution of structures of different shapes and sizes [24].

Another factor that contributes to the formation of porosity in the layered structure is the prevalence of surface contaminants in the raw material, such as moisture, impurities, and grease. The gas pores are usually trapped in the uppermost layer of the fusion zone, causing it to spread toward the top of the solidified weld pool. When thin oxide films form quickly on the surface of the weld pool, it easily absorb molecular hydrogen and moisture from the air, which then increases the amount of hydrogen present in the upper part of each layer. As a result, there is usually more trapped hydrogen and small micropores in the fusion line zone of each layer, which can grow and coalesce into larger pores when exposed to high temperatures. Consequently, larger pores are often observed along the fusion line zone between layers. Porosity is one of the most common and undesirable defects that greatly degrades weld properties such as strength and fatigue.

Our results show that the shielding gas flow rate affects the quality of the part. Increasing the gas flow rate reduces the porosity within the studied range. The single-scan track tests conducted in [24] show that even with single-scan tracks, the weld pool geometry is significantly dependent on the shielding gas flow conditions. Our experiments (Fig. 3) show that increasing the shielding gas flow rate within 8–14 l/min allows us to reduce the porosity in the deposited metal to almost zero. The pores trapped by the gas are spherical (Fig. 3). The pores develop throughout the process due to gas entrapment, supersaturation of dissolved gases, and chemical reaction within the weld pool, which leads to the formation of gaseous products [23, 24]. When the equilibrium gas pressure exceeds the sum of its hydrostatic, atmospheric, and capillary pressures, there is a high probability of the formation of trapped gas holes. Nucleating pores lead to vacancies [18, 21], allowing supersaturated gases to penetrate into the weld pool. When rapid cooling occurs, the pore nucleation sites can be captured by the weld pool. On the other hand, slower cooling rates allow these pores to enlarge and sometimes merge with neighboring pores. Further, our proposed mechanical grinding allows for further reduction of metal porosity by removing the defective layer after surfacing, as well as by removing the oxidized metal Fig. 4, 5.

Our experiments have shown that the wire feed affects the characteristics of the weld bead, including the weld bead height, weld bead width, and contact angle (Fig. 4, *b*). The effect of the wire feed on the weld bead width is difficult to control. Initially, the weld bead width reaches a maximum value, but then begins to decrease as the wire feed increases. This is because the contact angle continues to increase with wire feed, so insufficient wetting will have a negative effect on the weld bead. Arc current and voltage are other important elements in the *WAAM* optimization process. These are the main process control parameters that regulate the amount of heat supplied and dissipated, thereby affecting the weld deposition. It is important to prevent uneven bead deposition and poor surface roughness. In addition, excessive heat input may cause re-melting of previously deposited layers, which will adversely affect the microstructure, bead size, and its mechanical properties. It is important to optimize the current and voltage to improve the overall efficiency of the process. This allows for the optimal amount of heat required to melt the metals in the *WAAM* process. This minimizes defects such as wavy surface morphology, uneven layer deposits, and the time required for post-processing.

The microstructure of the weld beads' material shown in Fig. 6 consists of polygonal ferrite (*PF*) and intergranular lamellar pearlite (*P*), which is consistent with the work of other authors on *WAAM* with low-carbon wires [25]. Therefore, grain size analysis was performed on the *WAAM* material based on the micrographs of Fig. 6, *b*. The grain size was 25–35 μm, compared to traditional welding with *Sv-08G2S* wire [24–25]. The grain size usually increases as the beads grow with increasing distance from the base plate; this is due to the slower cooling away from the plate due to the decreasing influence of the heat removal effect [3–5, 22].

In *WAAM*, solidification is a major processing issue due to the advancement of the microstructure containing large columnar grains.

The mechanical properties of the weld beads are presented in Table 1. It is evident that additional machining of each bead improves the mechanical properties.

Table 2 presents the impact toughness test results for the test pieces. The impact toughness values with additional machining are higher due to the elimination of the deposited metal porosity, Fig. 7.

The results of ultrasonic hardening of the last deposited layer (Fig. 8) showed that it can smooth the weld tip profile, improve its microstructure, increase microhardness and introduce useful compressive residual stress into the surface layer. It is known that additional processing of welds allows creating compressive stresses in the surface layer, thereby increasing fatigue strength [28, 29]. The work [28] shows that residual compressive stress was created in the area of ultrasonic impact at a depth of 1.5–1.7 mm and a width of 15 mm.

Thus, our studies have shown that the use of an intermediate operation of machining of the weld bead improves the quality of the metal, and the final operation of ultrasonic processing of the upper bead (closing the additive growth process) increases the hardness of the surface layer. According to the results of studies [28, 29], it was found that ultrasonic processing of welds and weld beads reduces the quantitative values of technological residual stresses. In our further studies, we will continue the study in this matter in order to clarify the optimal processing parameters.

Conclusion

1. The relationship between the geometric dimensions of the surfacing beads and the porosity in the metal with and without interpass machining is established. It is shown that the metal formed by the new combined *WAAM* process has a higher set of mechanical properties compared to the metal obtained by the traditional *WAAM* technology.

2. It is established that the yield strength and ultimate strength of the metal formed by the combined *WAAM* process are 15–30 % higher than those obtained by the traditional *WAAM* process. The impact toughness values in impact bending tests of the metal formed by the combined *WAAM* process are 15–25 % higher than those obtained by the traditional *WAAM* process.

3. It is shown that ultrasonic hardening of the last deposited layer has a positive effect due to an increase in the microhardness of the surface layer of the metal and the formation of compressive stresses in it.

References

1. ISO/ASTM 52900. *Additive manufacturing – General principles – Fundamentals and vocabulary*. F42 Committee. West Conshohocken, PA, 2021. Available at: https://www.astm.org/Standards/ISOASTM52900.htm (accessed 2310.2024).

2. Gu D.D., Meiners W., Wissenbach K., Poprawe R. Laser additive manufacturing of metallic components: materials, processes and mechanisms. *International Materials Reviews*, 2012, vol. 57 (3), pp. 133–164. DOI: 10.1179/1743280411Y.0000000014.

3. Ngo T.D., Kashani A., Imbalzano G., Nguyen K.T., Hui D. Additive manufacturing (3D printing): a review of materials, methods, applications and challenges. *Composites, Part B: Engineering*, 2018, vol. 143, pp. 172–196. DOI: 10.1016/j.compositesb.2018.02.012.

4. Song Y.A., Park S. Experimental investigations into rapid prototyping of composites by novel hybrid deposition process. *Journal of Materials Processing Technology*, 2006, vol. 171 (1), pp. 35–40. DOI: 10.1016/j.jmatprotec.2005.06.062.

5. Wu B., Pan Z., Ding D., Cuiuri D., Li H., Xu J., Norrish J. A review of the wire arc additive manufacturing of metals: properties, defects and quality improvement. *Journal of Manufacturing Processes*, 2018, vol. 35, pp. 127–139. DOI: 10.1016/j.jmapro.2018.08.001.

6. Ahn D.G. Directed energy deposition (DED) process: state of the art. *International Journal of Precision Engineering and Manufacturing-Green Technology*, 2021, vol. 8 (2), pp. 703–742. DOI: 10.1007/s40684-020-00302-7.

7. Armstrong M., Mehrabi H., Naveed N. An overview of modern metal additive manufacturing technology. *Journal of Manufacturing Processes*, 2022, vol. 84, pp. 1001–1029. DOI: 10.1016/j.jmapro.2022.10.060.

8. Srivastava M., Rathee S., Patel V., Kumar A., Koppad P.G. A review of various materials for additive manufacturing: recent trends and processing issues. *Journal of Materials Research and Technology*, 2022, vol. 21, pp. 2612–2641. DOI: 10.1016/j.jmrt.2022.10.015.

9. Flynn J.M., Shokrani A., Newman S.T., Dhokia V. Hybrid additive and subtractive machine tools – research and industrial developments. *International Journal of Machine Tools and Manufacture*, 2016, vol. 101, pp. 79–101. DOI: 10.1016/j.ijmachtools.2015.11.007.

10. Nazir A., Gokcekaya O., Billah K.M., Ertugrul O., Jiang J., Sun J., Hussain S. Multi-material additive manufacturing: a systematic review of design, properties, applications, challenges, and 3D printing of materials and cellular metamaterials. *Materials & Design*, 2023, vol. 226, p. 111661. DOI: 10.1016/j.matdes.2023.111661.

11. Vatanparast S., Boschetto A., Bottini L., Gaudenzi P. New trends in 4D printing: a critical review. *Applied Sciences*, 2023, vol. 13 (13), p. 7744. DOI: 10.3390/app13137744.

12. Balanovskiy A.E., Karlina A.I., Kolosov A.D., Karlina Y.I. Study of the effect of nanomodifiers from silicon production wastes on morphological form of gray cast iron graphites. *CIS Iron and Steel Review*, 2021, vol. 21, pp. 64–69. DOI: 10.17580/cisisr.2021.01.11.

13. Wang C., Suder W., Ding J., Williams S. Bead shape control in wire based plasma arc and laser hybrid additive manufacture of Ti-6Al-4V. *Journal of Manufacturing Processes*, 2021, vol. 68, pp. 1849–1859. DOI: 10.1016/j.jmapro.2021.07.009.

14. Evans S.I., Wang J., Qin J., He Y., Shepherd P., Ding J. A review of WAAM for steel construction – manufacturing, material and geometric properties, design, and future directions. *Structures*, 2022, vol. 44, pp. 1506–1522. DOI: 10.1016/j.istruc.2022.08.084.

15. Kawalkar R., Dubey H.K., Lokhande S.P. Wire arc additive manufacturing: a brief review on advancements in addressing industrial challenges incurred with processing metallic alloys. *Materials Today: Proceedings*, 2022, vol. 50, pp. 1971–1978. DOI: 10.1016/j.matpr.2021.09.329.

16. Yelemessov K., Baskanbayeva D., Martyushev N.V., Skeeba V.Y., Gozbenko V.E., Karlina A.I. Change in the properties of rail steels during operation and reutilization of rails. *Metals*, 2023, vol. 13, p. 1043. DOI: 10.3390/met13061043.

17. Han C., Fang Q., Shi Y., Tor S.B., Chua C.K., Zhou K. Recent advances on high-entropy alloys for 3D printing. *Advanced Materials*, 2020, vol. 32 (26), p. 1903855. DOI: 10.1002/adma.201903855.

18. Diao M., Guo C., Sun Q., Jiang F., Li L., Li J., Xu D., Liu C., Song H. Improving mechanical properties of austenitic stainless steel by the grain refinement in wire and arc additive manufacturing assisted with ultrasonic impact treatment. *Materials Science and Engineering: A*, 2022, vol. 857, p. 144044. DOI: 10.1016/j.msea.2022.144044.

19. Hodonou C., Balazinski M., Brochu M., Mascle C. Material-design-process selection methodology for aircraft structural components: application to additive vs subtractive manufacturing processes. *International Journal of Advanced Manufacturing Technology*, 2019, vol. 103, pp. 1509–1517. DOI: 10.1007/s00170-019-03613-5.

20. Hodonou C., Kerbrat O., Balazinski M., Brochu M. Process selection charts based on economy and environment: subtractive or additive manufacturing to produce structural components of aircraft. *International Journal on Interactive Design and Manufacturing*, 2020, vol. 14, pp. 861–873. DOI: 10.1007/s12008-020-00663-y.

21. Huang C., Kyvelou P., Zhang R., Britton T.B., Gardner L. Mechanical testing and microstructural analysis of wire arc additively manufactured steels. *Materials & Design*, 2022, vol. 216, p. 110544. DOI: 10.1016/j.matdes.2022.110544.

22. Balanovskiy A.E., Astafyeva N.A., Kondratyev V.V., Karlina A.I. Study of mechanical properties of C-Mn-Si composition metal after wire-arc additive manufacturing (WAAM). *CIS Iron and Steel Review*, 2021, vol. 22, pp. 66–71. DOI: 10.17580/cisisr.2021.02.12.

23. Ermakova A., Mehmanparast A., Ganguly S., Razavi N., Berto F. Investigation of mechanical and fracture properties of wire and arc additively manufactured low carbon steel components. *Theoretical and Applied Fracture Mechanics*, 2020, vol. 109, p. 102685. DOI: 10.1016/j.tafmec.2020.102685.

24. Balanovskiy A.E., Astafyeva N.A., Kondratyev V.V., Karlina Yu.I. Study of impact strength of C-Mn-Si composition metal after wire-arc additive manufacturing (WAAM). *CIS Iron and Steel Review*, 2022, vol. 24, pp. 67–73. DOI: 10.17580/cisisr.2022.02.10.

25. Karlina A.I., Kondratyev V.V., Balanovskiy A.E., Astafyeva N.A., Yamshchikova E.A. Porosity reduction in metal with hybrid wire and arc additive manufacturing technology (WAAM). *CIS Iron and Steel Review*, 2024, vol. 27, pp. 91–95. DOI 10.17580/cisisr.2024.01.14.

26. Kyvelou P., Slack H., Mountanou D.D., Wadee M.A., Britton T.B., Buchanan C., Gardner L. Mechanical and microstructural testing of wire and arc additively manufactured sheet material. *Materials & Design*, 2020, vol. 192, p. 108675. DOI: 10.1016/j.matdes.2020.108675.

27. Lin Z., Goulas C., Ya W., Hermans M.J.M. Microstructure and mechanical properties of medium carbon steel deposits obtained via wire and arc additive manufacturing using metal-cored wire. *Metals*, 2019, vol. 9 (6), p. 673. DOI: 10.3390/met9060673.

28. Cao Y., Zhang Y., Ming W., He W., Ma J. Review: The metal additive-manufacturing technology of the ultrasonic-assisted wire-and-arc additive-manufacturing process. *Metals*, 2023, vol. 13, p. 398. DOI: 10.3390/met13020398.

29. Kumar S., Wu C.S., Padhy G.K., Ding W. Application of ultrasonic vibrations in welding and metal processing: a status review. *Journal of Manufacturing Processes*, 2017, vol. 26, pp. 295–322. DOI: 10.1016/j.jmapro.2017.02.027.

30. Shtayger M.G., Balanovskiy A.E., Kargapoltsev S.K., Gozbenko V.E., Karlina A.I., Karlina Yu.I., Govorkov A.S., Kuznetsov B.O. Investigation of macro and micro structures of compounds of high-strength rails implemented by contact butt welding using burning-off. *IOP Conference Series: Materials Science and Engineering*, 2019, vol. 560 (1), p. 012190. DOI: 10.1088/1757-899X/560/1/012190.

31. Balanovskiy A.E., Shtayger M.G., Karlina A.I., Kargapoltsev S.K., Gozbenko V.E., Karlina Yu.I., Govorkov A.S., Kuznetsov B.O. Surface hardening of structural steel by cathode spot of welding arc. *IOP Conference Series: Materials Science and Engineering*, 2019, vol. 560 (1), p. 012138. DOI: 10.1088/1757-899X/560/1/012138.

32. Haden C.V., Zeng G., Carter F.M., Ruhl C., Krick B.A., Harlow D.G. Wire and arc additive manufactured steel: tensile and wear properties. *Additive Manufacturing*, 2017, vol. 16, pp. 115–123. DOI: 10.1016/j.addma.2017.05.010.

33. Dirisu P., Ganguly S., Mehmanparast A., Martina F., Williams S. Analysis of fracture toughness properties of wire + arc additive manufactured high strength low alloy structural steel components. *Materials Science and Engineering: A*, 2019, vol. 765, p. 138285. DOI: 10.1016/j.msea.2019.138285.

34. Skeeba V.Yu., Ivancivsky V.V., Kutyshkin A.V., Parts K.A. Hybrid processing: the impact of mechanical and surface thermal treatment integration onto the machine parts quality. *IOP Conference Series: Materials Science and Engineering*, 2016, vol. 126 (1), p. 012016. DOI: 10.1088/1757-899x/126/1/012016.

35. Efremenkov E.A., Martyushev N.V., Skeeba V.Yu., Grechneva M.V., Olisov A.V., Ens A.D. Research on the possibility of lowering the manufacturing accuracy of cycloid transmission wheels with intermediate rolling elements and a free cage. *Applied Sciences*, 2022, vol. 12 (1), p. 5. DOI: 10.3390/app12010005.

36. Martyushev N.V., Skeeba V.Yu. The method of quantitative automatic metallographic analysis. *Journal of Physics: Conference Series*, 2017, vol. 803 (1), p. 012094. DOI: 10.1088/1742-6596/803/1/012094.

37. Skeeba V.Yu., Ivancivsky V.V. Reliability of quality forecast for hybrid metal-working machinery. *IOP Conference Series: Earth and Environmental Science*, 2018, vol. 194 (2), p. 022037. DOI: 10.1088/1755-1315/194/2/022037.

38. Zverev E.A., Skeeba V.Yu., Skeeba P.Yu., Khlebova I.V. Defining efficient modes range for plasma spraying coatings. *IOP Conference Series: Earth and Environmental Science*, 2017, vol. 87 (8), p. 082061. DOI: 10.1088/1755-1315/87/8/082061.

39. Skeeba V.Yu. Gibridnoe tekhnologicheskoe oborudovanie: povyshenie effektivnosti rannikh stadii proektirovaniya kompleksirovannykh metalloobrabatyvayushchikh stankov [Hybrid process equipment: improving the efficiency of the integrated metalworking machines initial designing]. *Obrabotka metallov (tekhnologiya, oborudovanie, instrumenty) = Metal Working and Material Science*, 2019, vol. 21, no. 2, pp. 62–83. DOI: 10.17212/1994-6309-2019-21.2-62-83.

40. Borisov M.A., Lobanov D.V., Yanyushkin A.S., Skeeba V.Yu. Issledovanie protsessa avtomaticheskogo upravleniya smenoi polyarnosti toka v usloviyakh gibridnoi tekhnologii elektrokhimicheskoi obrabotki korrozionnostoikikh stalei [Investigation of the process of automatic control of current polarity reversal in the conditions of hybrid technology of electrochemical processing of corrosion-resistant steels]. *Obrabotka metallov (tekhnologiya, oborudovanie, instrumenty) = Metal Working and Material Science*, 2020, vol. 22, no. 1, pp. 6–15. DOI: 10.17212/1994-6309- 2020-22.1-6-15.

41. Mamadaliev R.A., Bakhmatov P.V., Martyushev N.V., Skeeba V.Yu., Karlina A.I. Influence of welding regimes on structure and properties of steel 12KH18N10T weld metal in different spatial positions. *Metallurgist*, 2022, vol. 65 (11–12), pp. 1255–1264. DOI: 10.1007/s11015-022-01271-9.

42. Balanovsky A.E., Shtayger M.G., Kondrat'ev V.V., Van Huy V., Karlina A.I. Plasma-arc surface modification of metals in a liquid medium. *IOP Conference Series: Materials Science and Engineering*, 2018, vol. 411 (1), p. 012013. DOI: 10.1088/1757-899X/411/1/012013.

43. Ivanchik N.N., Balanovsky A.E., Shtayger M.G., Sysoev I.A., Karlina A.I. Capability enhancement of production of activating fluxes for arc welding using ultradispersed products of silicon waste processing. *IOP Conference Series: Materials Science and Engineering*, 2018, vol. 411 (1), p. 012035. DOI: 10.1088/1757-899X/411/1/012035.

44. Karlina A.I., Karlina Y.I., Gladkikh V.A. Studying the microstructure, phase composition, and wear resistance of alloyed layers after laser surface melting of low-carbon steel 20. *Metallurgist*, 2024, vol. 68, p. 757–766. DOI: 10.1007/s11015-024-01782-7.

45. Karlina A.I., Karlina Y.I., Kondratiev V.V., Kononenko R.V., Breki A.D. Study of wear of an alloyed layer with chromium carbide particles after plasma melting. *Crystals*, 2023, vol. 13 (12), p. 1696. DOI: 10.3390/cryst13121696.

Conflicts of Interest

The authors declare no conflict of interest.